Sorption and Redox Speciation of Plutonium at the Illite Surface

Nidhu Lal Banik, Remi Marsac, Johannes Lützenkirchen, Alexandre Diascorn, Kerstin Bender, Christian M. Marquardt, Horst Geckeis

Sorption and Redox Speciation of Plutonium at the Illite Surface

Nidhu lal Banik[‡*], Rémi Marsac[‡†], Johannes Lützenkirchen[‡], Alexandre Diascorn[‡#], Kerstin Bender[‡], Christian Michael Marquardt[‡] and Horst Geckeis[‡]

[‡]Institut für Nukleare Entsorgung, Karlsruhe Institute of Technology, P.O. Box 3640, D-76021 Karlsruhe, Germany

ABSTRACT. The geochemical behavior of Pu strongly depends on its redox speciation. In this study we investigated Pu sorption onto Na-illite, a relevant component of potential host rocks for high-level nuclear waste repositories, under anaerobic conditions. When contacting Pu (85% Pu(IV), 11% Pu(V) and 4% Pu(III); $8\times10^{-11} < [Pu]_{tot}/M < 10^{-8}$) with illite in 0.1 M NaCl at pH between 3 and 10, Pu uptake was characterized by log $R_d > 4$ (R_d: distribution coefficient in L kg^{-1}). Small amounts of aqueous Pu(V) were detected in solution on contact with illite after one week which is not expected to be stable at the measured redox potentials (Eh) in our experiments. This observation suggests time dependent reduction of Pu(V) to Pu(IV). After one year, log R_d values had increased compared to those after one week due to the reduction of weakly adsorbing Pu(V). For pH < 5, Pu(IV) and Pu(III) coexisted in solution under our experimental conditions, showing that Pu(IV) reduction to Pu(III) occurred in the illite suspension. Taking (i) surface complexation constants determined for Eu(III)-illite interaction (with redox insensitive Eu(III) as a chemical analogue to Pu(III)), (ii) the known constant for Pu(III)/Pu(IV) redox transition, and (iii) measured Eh and pH, overall Pu uptake was well predicted.

INTRODUCTION

Due to its high radiotoxicity and the very long half-lives of some isotopes, plutonium (Pu) is an important element in the context of nuclear waste disposal. Under environmentally relevant conditions, Pu can occur in the oxidation states +III, +IV, +V and +VI. As the geochemical behavior of Pu, such as solubility and mobility, strongly depends on its redox state,[1,2] thermodynamic speciation calculations need to account for Pu redox speciation.

Several studies have shown that actinide redox chemistry is affected by interaction with mineral surfaces. The evaluation of Pu sorption data is particularly challenging as frequently a mixture of Pu redox states is found in solid/liquid systems (i.e. at the surface and/or in solution). In the presence of a mineral, rates for abiotic redox reactions range from a few hours to a few months and depend on the mineral type, pH, Pu concentration and initial Pu redox state, which further complicates data interpretation.[3-8] Generally, under ambient (air) atmosphere, when adding Pu(IV), Pu(V) or Pu(VI) to a mineral suspension (hematite, goethite, magnetite,[5-10] quartz,[11] montmorillonite,[3,4] kaolinite[12]), Pu(IV) is found at the mineral surface whereas very often Pu(V) prevails in solution. Similar observations were made for neptunium (Np) and illite under slightly reducing conditions.[13] However, the standard redox potential of the Np(V)/Np(IV) couple ($E^0_{NpO_2^+/Np^{4+}} = 0.604\ V$) is lower than that of the Pu(V)/Pu(IV) pair ($E^0_{PuO_2^+/Pu^{4+}} = 1.031\ V$).[14] Pu sorption to minerals under reducing conditions, where Pu(III) should prevail, has been probed less frequently. Under inert ($N_{2(g)}$ or $Ar_{(g)}$) atmosphere, magnetite was shown to reduce Pu(V) to Pu(III) at pH = 6 and 8, whereas Pu(III) was not observed under ambient atmosphere.[7,15] In the presence of kaolinite and $NH_2OH{\cdot}HCl$ added as a weaker reducing agent than magnetite, Pu(III) was oxidized to Pu(IV) at pH > 6.[16] Banik et al.[13] noticed the presence of Pu(III) at pH = 1 in the solution when in contact with kaolinite under ambient atmosphere, which is explained by the

45 higher stability of Pu(III) at low pH. All these studies suggest that Pu redox speciation is strongly
46 affected by the redox conditions in the investigated system and the presence of mineral surfaces.
47 In recent studies, it was shown that the overall uptake of redox sensitive actinides can be
48 quantitatively predicted by taking into account the uptake of the individual redox states and the
49 measured redox potentials, i.e. the negative logarithm of (apparent) electron activity, pe. In the
50 case of Np, the high stability of Np(IV) surface complexes significantly extended the
51 predominance field of Np(IV) at the illite surface as compared to that valid for the pure aqueous
52 solution. This finding explains the prevalence of Np(V) in solution and of Np(IV) at the surface.
53 Overall R_d values obtained for the sorption of Np thus lie between that of penta- and tetravalent
54 actinides.[13] The same modeling approach was applied to simulate Pu sorption and redox
55 speciation at the kaolinite surface.[17] Lanthanides and actinides are known to exhibit similar
56 chemical behavior for a given redox state.[1,2,18] Because separate uptake data for the four distinct
57 Pu redox states are not available (and will be difficult to obtain experimentally), sorption data for
58 europium(III) or americium(III) (Eu^{3+}/Am^{3+}), thorium(IV) (Th^{4+}), neptunium(V) (NpO_2^+) and
59 uranium(VI) (UO_2^{2+}) were used to estimate sorption data of the respective Pu redox states. As
60 both Pu(IV) and Pu(III) show strong sorption to mineral surfaces over a wide range of pH
61 conditions, Pu(IV) and Pu(III) predominance fields are expected to be less affected by the
62 presence of mineral surfaces than in the case of Np,[13,17] where the sorption behavior of the redox
63 species +V and +IV are clearly different.
64 Pu sorption onto purified illite[13] in 0.1 M NaCl is experimentally investigated in the present study
65 under anaerobic conditions in order to verify the reliability and applicability of those previously
66 reported modeling approaches. Pu sorption to illite is interpreted involving known data on redox
67 and adsorption equilibria within the 2 site protolysis non-electrostatic surface complexation and
68 cation exchange (2 SPNE SC/CE) model[19-21] to quantify Pu surface speciation.

MATERIALS AND METHODS

All chemicals (pro analytical quality or better) were obtained from Merck (Darmstadt, Germany) or Riedel de Haen (Seelze, Germany). Solutions were prepared with de-ionized "MilliQ" water (specific resistivity, 18.2 MΩ cm^{-1}). The purified Na-illite was provided within the EC project CP CatClay (www.catclay.org). The source material derives from lacustrine continental sediments deposited at the Upper Eocene (~ -35 Ma) in the basin of Le Puy en Velay (Massif Central, France). The purification procedures and the characterization of the purified illite (<63 μm) were previously given in detail[13] and will not be repeated here. Note that in the last step of the purification, the clay suspension was freeze dried, to exclude bacterial activity.

Plutonium and Europium stock solution. A ^{238}Pu stock solution was prepared from a solution of plutonium dissolved in concentrated nitric acid, which was fumed three times by 0.1 M $HClO_4$, in order to remove nitrate and organic traces. The concentration of the Pu stock solution was 3.9×10^{-5} M in 0.1 M $HClO_4$. A more dilute solution ([Pu] = 1.9×10^{-6} M) in 0.1 M $HClO_4$ was prepared from that stock solution – however, the solution was left under argon atmosphere for several months before dilution - to perform experiments at low Pu(IV) concentration. The concentrations of ^{238}Pu in solution were determined by liquid scintillation counting (LSC) using the scintillation cocktail Ultima Gold XR with a liquid scintillation analyzer (Tri-Carb 3110TR). In addition, the stock solution of ^{238}Pu were checked by ICP-MS measurements and the results were in excellent agreement with LSC measurements.

Eu(III) was investigated as a chemical analogue of Pu(III). A radiotracer solution was purchased from Amersham International (total Eu concentration: 6.0×10^{-4} M) with isotopic composition: ^{151}Eu (83%), ^{152}Eu (13%, $t_{1/2}$ = 13.33a), ^{153}Eu (4%). ^{152}Eu is a β-, γ-emitter and can be

conveniently analyzed by γ-counting. In the present study, precise determination of dissolved ^{152}Eu concentration, was performed using a Perkin Elmer Wallac gamma counter (Wizard 1480).

Plutonium redox state analysis by liquid-extraction methods. The Pu redox state distribution in the diluted ^{238}Pu stock solution (1.9×10^{-6} M; in 0.1 M $HClO_4$) and in the supernatant of Pu-illite samples prepared for $[Pu]_{tot} = 10^{-8}$ M was determined by liquid-liquid extraction.[22,23] Two different complexing agents, 0.025 M PMBP in toluene and 0.5 M HDEHP in xylene, were used (PMBP: 4-benzoyl-3-methyl-1-phenyl-pyrozolin-5-one; HDEHP: phosphoric acid bis-(2-ethyl-hexyl) ester).[22,23] The aqueous Pu-sample solution mixed with the organic extractant was stirred for 10 minutes and then centrifuged for 10 minutes at 4000 rounds per minute (rpm). After separation of the aqueous and the organic phases, activities were measured in each phase by LSC. Four different extractions were made separately. With PMBP at pH 0 (extraction 1), Pu(IV) is extracted into the organic phase, while Pu(III), Pu(V), Pu(VI) and polymers remain in the aqueous phase. With PMBP at pH 0 and 0.02 M $Cr_2O_7^{2-}$ (extraction 2), Pu(III) and Pu(IV) are extracted into the organic phase, while Pu(V), Pu(VI) and polymers remain in the aqueous phase. With HDEHP at pH 0 (extraction 3), Pu(IV) and Pu(VI) are extracted into the organic phase, while Pu(III), Pu(V) and polymers remain in the aqueous phase. With HDEHP at pH 0 and 0.02 M $Cr_2O_7^{2-}$ (extraction 4), Pu(III), Pu(IV), Pu(V) and Pu(VI) are extracted into the organic phase while polymers remain in the aqueous phase. All steps for the separation of the different oxidation states of plutonium and the calculation leading to the aqueous redox speciation of Pu are outlined in the supporting information (Figure S1). The uncertainty of the method is conservatively estimated to be ±10%, and includes the pipetting error, phase separation of mixture, quenching factor of the analyte solution (color) for the LSC

measurements and the variability observed for different extraction experiments. The diluted ^{238}Pu stock solution contained 85% Pu(IV), 11% Pu(V) and 4% Pu(III). Seemingly, the Pu(VI) expected from the preparation step is not stable at low concentrations under the present experimental conditions, which was also observed by Neck et al.[24]

Determination of pH and Eh. The pH in the clay suspensions was measured by an Orion 525A (pH meter) and a Ross electrode calibrated with 4 standard buffers (pH 3, 5, 7 and 9; Merck). The error in pH measurements is ±0.05. The redox potentials in the clay suspensions were measured using an Orion 525A (E_h meter) and a Pt electrode combined with the Ag/AgCl reference system (Metrohm). Raw data were converted into Eh vs. standard hydrogen electrode (SHE) by correcting for the potential of the reference electrode. Eh was converted to the apparent electron activity, $pe = -\log a_{e^-} = 16.9 \times Eh(V)$ at 25°C. A commercial redox-buffer (220 mV, Schott instruments) was used for calibration. After having stirred the suspension, a time span of 15 min was allowed for all Eh measurements. Uncertainties in Eh measurements are ±50 mV.[15,24]

Batch sorption experiments. All sorption studies were performed as batch type experiments. The effect of pH was investigated for an initial Pu concentration ($[Pu]_{tot}$) of 8×10^{-11} M. In addition, the effect of $[Pu]_{tot}$ was investigated for $8\times10^{-11} < [Pu]_{tot} < 10^{-8}$ M, at pH ≈ 4, 7 and 10. Batch experiments were carried out in 40 mL polypropylene centrifuge tubes at room temperature in an argon glove box (< 1 ppm O_2, absence of CO_2). The suspension volume was 25 mL. At a solid to liquid ratio of 2 g L^{-1}, the suspensions were preconditioned in 0.1 M NaCl under continuous shaking for 4-5 days to achieve a given target pH value by adding 0.1 M HCl or 0.1 M NaOH. After adding Pu to the illite suspension, pH was adjusted again to the required pH

of the sample. Neither pH nor Eh buffers were used. The samples were closed and shaken end-over-end. After one week, pH and Eh were measured in the suspension and an aliquot of each sample was transferred to special centrifuge tubes (Beckmann, Recorder No.: 356562) and centrifuged (Beckmann Coulter XL-90 K) at 90,000 rpm (~700,000 g max) for one hour. The supernatant was analyzed for dissolved Pu by LSC. Samples were kept in the glovebox without any pH adjustment and the procedure was repeated after one year of contact time. Results from the batch experiments are expressed throughout as distribution coefficients (R_d in L kg^{-1}), calculated by the following equation:

$$R_d = \left([Pu]_{tot}/[Pu]_{aq} - 1\right) \times V/m \quad (1)$$

where $[Pu]_{aq}$ and $[Pu]_{tot}$ (M) are the dissolved (final) equilibrium and total (initial) concentrations of Pu, respectively. The term V/m corresponds to the aqueous solution volume to illite mass ratio (L kg^{-1}). According to our experimental results (see below), an uncertainty of ±0.2 (standard deviation) is assigned to log R_d, although it could be larger according to comparable studies where more than 99% uptake is obtained.[20,21] Under such conditions, larger uncertainties are induced by analytical constraints.

Batch Eu sorption experiments were performed for $[Eu]_{tot} = 3\times10^{-9}$ M applying the same protocol as for Pu, except that Eh was not recorded because Eu is not redox sensitive under our experimental conditions. After one week contact time and subsequent ultracentrifugation, the supernatant was analyzed for dissolved Eu by γ-spectrometry. The latter procedure was repeated after 4 months to estimate potential aging effects on Eu sorption to illite. No aging effect is observed for Eu(III) under our experimental conditions (see Fig. S2).

Thermodynamic modeling. pe-pH diagrams for Pu were constructed using PhreePlot,[25] which contains an embedded version of the geochemical speciation program PHREEQC.[26] Thermodynamic constants for Pu and Eu aqueous speciation were taken from the NEA thermodynamic database.[14] The specific ion interaction theory (SIT)[27] was used for the calculation of the activity coefficients of aqueous species. In case of gaps in the Pu database, data for analogues were chosen (i.e. Eu(III), Np(IV), Np(V) and U(VI) for the respective Pu redox states). Auxiliary reactions and constants (from the SIT database) are provided with PHREEQC (sit.dat file). The 2 SPNE SC/CE model was used to simulate Pu and Eu sorption to illite, where the cation exchange capacity (CEC) and the strong site density of the illite surface are considered equal to 0.225 eq kg^{-1} and 2×10^{-3} mol kg^{-1}, respectively.[19-21] Only the strong sites within the 2 SPNE SC/CE model are considered in the adsorption calculations. The weak sites play a negligible role in our experiments, since a maximum Pu loading of only 5×10^{-6} mol kg^{-1} (i.e. for $[Pu]_{tot} = 10^{-8}$ M) is investigated. A complete summary of the thermodynamic database, SIT coefficients and parameters for the 2SPNE SC/CE model is given in the supporting information (Table S1, S2 and S3).

RESULTS AND DISCUSSION

Pu sorption to illite in 0.1 M NaCl. pH-pe data recorded after 1 week and 1 year equilibration time in the Pu-illite suspension in 0.1 M NaCl solution are plotted in Figure 1 together with the calculated predominance pH-pe diagram for dissolved Pu. The solid lines correspond to equal amounts of two Pu redox states. Large symbols indicate the samples where the supernatant was additionally analyzed by liquid extraction ($[Pu]_{tot} = 10^{-8}$ M; see Table S4 and

184 S5 for more information regarding these samples). Data are compared to those reported for the
185 Np-illite system at similar metal ion concentration (3×10^{-8} M) and after contact times between 7
186 and 63 days[13] and agree well within experimental uncertainties. Between 1 week and 1 year, pH
187 may slightly evolve due to further buffering of illite, since no pH-buffer was used. An increase in
188 pe values is also observed for the batch series prepared to study the effect of pH ($[Pu]_{tot}=8\times10^{-11}$
189 M), which is potentially due to the presence of undetectable traces of $O_{2(g)}$ (i.e. < 1 ppm) during
190 sample handling or storage over the 1 year period. This has, however, no impact on our
191 conclusions, which are based on the finally established pe and pH values. Batch series conducted
192 for pH ≈ 4, 7 and 10 ($8\times10^{-11} < [Pu]_{tot} < 10^{-8}$ M) exhibit quite stable pe values with time, which
193 suggests no significant $O_{2(g)}$ contamination or microbial activity over the 1 year period.
194 Significant amounts of Pu(III) are expected in the aqueous phase below pH ≈ 5 whereas Pu(IV)
195 should prevail above pH ≈ 6 according to the calculations and taking pe data uncertainties into
196 account. However, in sorption experiments ($[Pu]_{tot} = 10^{-8}$ M) performed over a period of 1 week,
197 we found at pH = 4.3 about 90% of the Pu in the supernatant aqueous phase being pentavalent
198 (Table S5). In analogy to the observed behavior of Np(V), the Pu(V) sorption to illite at pH = 4.3
199 is considered negligible and remains in solution. Pu(IV), like other tetravalent actinide ions, is
200 expected to be almost completely sorbed (see e.g. the literature Np(V)- and Th(IV)-illite sorption
201 data in Fig. S2 and Fig. S3, respectively).[21,28] In our sample, only 7% of the total Pu remain in
202 solution. Therefore, Pu(V) represents ~6% of the total Pu amount in the system, which
203 corresponds to about half of Pu(V) initially present in the ^{238}Pu stock solution (11% of Pu(V)). At
204 pH = 6.9, only 3% of Pu remain in solution after ultracentrifugation with 20% Pu(V), while at pH
205 = 10 the redox state of Pu in solution is entirely +IV after 1 week. We attribute this finding to a
206 time dependent Pu(V) reduction in our system which apparently accelerates with increasing pH.
207 A similar time dependent reduction of Pu(V) to Pu(IV) was observed in presence of hematite and

goethite,[6,8,9] montmorillonite[3,4] and other minerals.[3,11] Reanalysis after 1 year revealed stronger Pu sorption and Pu redox states ($[Pu]_{tot}$ = 10^{-8} M) in the aqueous phase are now in better agreement with thermodynamic considerations. At pH = 4.3, 22 ± 10% Pu(III), 85 ± 10% Pu(IV) and no Pu(V) is detected. According to the measured pe data range (6.2 ± 0.9), between 88% and 100% of Pu(III) are predicted to exist in solution and 0-12% Pu(IV) which qualitatively agrees with the experimental results. At pH = 6.9 and 9.3, Pu(IV) clearly dominates and no significant amounts of Pu(V) or Pu(III) could be found, as calculated using the measured pe values. We have to emphasize that the observed time dependent redox reaction relates to only the initial Pu(V), i.e. a small fraction of the total Pu. The major Pu fraction is sorbed, either as Pu(III) or Pu(IV). However, those small variations have a significant impact on R_d values, as will be discussed below. It is also understood that the time for attaining overall equilibrium might be shorter than 1 year. Such a long waiting period has been chosen in order to make sure that equilibrium has established similar to the procedure proposed in a previous Pu-montmorillonite sorption study.[3]

Figure 2a shows Pu sorption to illite (R_d: distribution coefficient in L kg^{-1}) as a function of pH after 1 week and 1 year contact time for $8\times10^{-11} < [Pu]_{tot} < 10^{-8}$ M. While Pu uptake by illite is always high, R_d values after 1 week are lower for pH < 7 than after 1 year (except for some data at pH = 4.3, which will be discussed later). This is consistent with the disappearance of Pu(V), which sorbs weakly compared to Pu(IV) and Pu(III). Earlier studies dealing with Np(V)-illite interaction[13] revealed faster redox reactions and equilibrium was assumed to be established after 1 week. However, under those pH/pe conditions, Np prevails in pentavalent state in solution according to measurements and geochemical calculations which makes Np different from Pu. Consequently, R_d values for Np are smaller than those observed for Pu, so that slight variations in redox have less impact on R_d values for Np as compared to those for Pu. Slow redox kinetics for Np can thus not be excluded but the error related to kinetics might have been negligible

232 compared to, for instance, experimental uncertainty on pe. Other mechanisms such as
233 incorporation reactions or sorption by secondary phases might also explain slow reaction rates.
234 Such reactions have been reported for mineral phases with high surface dynamics such as calcite,
235 apatite and brucite which can be estimated from known mineral dissolution rates (see e.g. [2,29]).
236 By contrast, dissolution rates of clays (e.g., for smectite)[30] are slow and actinide incorporation in
237 clays has rarely been observed in laboratory studies,[2] except at high pH (i.e. pH > 12)[31] or in
238 coprecipitation studies.[32] Moreover, sorption of redox inactive radionuclides such as Eu(III) and
239 Am(III) to clays is relatively fast and proceeds within less than 1 week.[20,21] For instance, as
240 shown in Figure S2, Eu(III) sorption to illite does not evolve significantly between 1 week and 4
241 months equilibration time. Although incorporation processes of Pu(III/IV/V) in illite cannot be
242 entirely excluded for the 1 year old samples, they very likely play a minor role with respect to the
243 increase in R_d with time compared to Pu(V) reduction to Pu(IV).
244 Given the general agreement of results of thermodynamic calculations with experimentally
245 determined Pu redox states in solutions in contact with illite for 1 year, we assume establishment
246 of an overall equilibrium. Pu uptake by illite after 1 year contact time (Figure 2a) is characterized
247 by a constant log $R_d = 5.2 \pm 0.2$ (1σ) for pH > 5. Sorption of tetravalent elements onto minerals is
248 reported to be widely insensitive to pH as for Sn(IV) and Th(IV) sorption to illite shown in
249 Figure S3.[20,21] Pu sorption data (log R_d) for pH > 5 are plotted in figure 2b against the logarithm
250 of the final aqueous Pu concentration (log $[Pu]_{aq}$). $[Pu]_{aq}$ in presence of illite is close to or below
251 the solubility limit of Pu(IV) in equilibrium with $PuO_{2(am,hydr)}$ (i.e. log $[Pu]_{aq} \approx -10.4$, for pH >
252 6).[24] Precipitation of $PuO_{2(am,hydr)}$ can thus be excluded. Figure 2b shows that log R_d is
253 independent of the total Pu concentration and does not vary with log $[Pu]_{aq}$ for pH > 5. This is in
254 line with previous studies of Th(IV) sorption onto illite-containing argillaceous rocks (where
255 illite was shown to be the major adsorbant), where an ideal Th(IV) sorption was observed for a

similar range of Th(IV) to clay concentration ratios for 7 < pH < 8.[33,34] Lower sorption of Pu at pH = 3 (figure 2a) can be attributed to the prevalence of less sorbing Pu(III), which is more stable at low pH (Fig. 1). Different sorption behavior of tri- and tetravalent metal ions at such low pH is well known for e.g. Eu(III) and Th(IV).[19-21] Scattering R_d data obtained for pH = 4.3 might suggest a concentration-dependent uptake of Pu (figure 2b). However, this is very unlikely because investigated surface coverages (between 4×10^{-8} and 5×10^{-6} mol of Pu per kg of illite) are below the saturation of any high affinity sites for illite, where an ideal sorption behavior has been evidenced for many metal ions (see e.g. Figure 2 in reference 13, and references therein). Instead, log R_d variations at pH = 4.3 might be explained by the observed uncertainties of measured pe data close to the Pu(IV)/Pu(III) borderline in Fig. 1 and possible slight heterogeneities in illite samples (e.g. with regard to Fe(II)-content). Log R_d seems to increase with pe (Fig. 2c), consistent with a transition between Pu(III) and Pu(IV), even though a clear conclusion is hampered by the relatively large uncertainty of measured pe data. This observation will be supported by surface complexation modeling (see below).

Modeling results. As previously found for Np(V) interaction with illite and Pu sorption to kaolinite and hematite, the redox speciation of actinides is influenced by the formation of surface complexes.[13,17,35] Equation 2 provides a simple approach to determine the stability field of Pu(IV) and Pu(III) at a mineral surface:[17]

$$\{Pu(IV)/Pu(III)\}_{surf} = \{Pu(IV)/Pu(III)\}_{aq} + (\log R_d(Pu(III)) - \log R_d(Pu(IV))) \qquad (2)$$

278 $\{Pu(IV)/Pu(III)\}_{aq}$ can be calculated by the Nernst equation (see reference 17 for details) and the
279 redox borderline in aqueous solution (Figures 1 and 3a) denotes an equimolar Pu(III)/Pu(IV)
280 ratio. $\{Pu(IV)/Pu(III)\}_{surf}$ refers to the corresponding redox speciation at the illite surface. Log
281 R_d(Pu(III)) and log R_d(Pu(IV)) values in eq. 2 represent the respective individual uptake of the
282 two Pu redox states under the same physico-chemical conditions and are expressed as distribution
283 coefficients (denoted as K_d in reference 17). As R_d values for Pu(III) and Pu(IV) are difficult to
284 determine separately, we took in a first approach existing models for Eu(III)[19] and Np(IV)[13] to
285 estimate sorption of Pu(III) and Pu(IV), respectively. The resulting Pu(IV)/Pu(III) borderline is
286 shown in Figure 3a as a dashed bold red line. pH-edges for Eu(III) and Np(IV) sorption onto illite
287 in 0.1 M NaCl calculated with the 2 SPNE SC/CE model are shown in Figure 3b. For pH < 7,
288 Eu(III) sorption to illite is weaker than that of Np(IV). At this low pH outer-sphere sorption (ion
289 exchange) dominates for Eu(III). Due to the higher thermodynamic stability of actinide(IV)
290 surface complexes in this area, the predominance field of Pu(IV) is enlarged at the illite surface
291 and overlaps with the stability field of Pu(III) in the aqueous phase. For pH > 7, Eu(III) and
292 Np(IV) uptake are almost equal. As a consequence, the Pu(IV)/Pu(III) borderline at the illite
293 surface coincides with that in solution ($\{Pu(IV)/Pu(III)\}_{surf} \approx \{Pu(IV)/Pu(III)\}_{aq}$). The pH-pe
294 values measured after 1 year in the Pu-illite suspensions are also plotted in Figure 3a. According
295 to these estimations, Pu(IV) is expected to prevail (or, at least, to be present in significant
296 amounts) at the illite surface in all samples. For pH > 6, Pu(III) becomes negligible and Pu
297 speciation in solution and at the illite surface is controlled by Pu(IV). For pH < 5, the overall Pu
298 uptake by illite is predicted to lie between that of Eu(III) and Np(IV), which is indeed the case
299 according to experimental data (Figure 3b).
300 We performed Eu(III) uptake experiments in 0.1 M NaCl ($[Eu]_{tot} = 3\times10^{-9}$ M) for 3 < pH < 9 with
301 our illite batch in order to exclude the possible impact of different clay mineral batches with

slightly variable surface properties (e.g. due to application of different purification procedures) on sorption. As shown in Fig. S2, the 2 SPNE SC/CE model with the set of surface complexation constants determined for Eu(III)[19] predicts the experimental data fairly well without any parameter adjustment. As discussed previously,[13] the estimated surface complexation constants for Np(IV) are based on various assumptions and affected by relatively large uncertainties (i.e. an error of ± 1.1 on log K values for the 2 SPNE SC/CE model) for various reasons and are restricted to 4 < pH < 10. According to our pe measurements, only Pu(IV) is expected in solution for pH > 6 after 1 year, as confirmed by Pu redox state analysis. According to our calculations, no redox state of Pu other than Pu(IV) should be present at the surface for pH > 6. We, therefore, conclude that our data are representative of the sorption behavior of Pu(IV) and that they can be used to derive more precise surface complexation constants for tetravalent Pu (Table S2). The respective constants lie below those reported earlier for Np(IV) but still within the uncertainty ranges (Figure S3). To describe Pu(IV) sorption at pH < 4 (Figure 3b) we included the $\equiv SOPuOH^{2+}$ surface complex in order to be consistent with sorption data for other tetravalent cations (Th(IV)[21] and Sn(IV)[20], see Figure S3) that do not exhibit a R_d decrease at pH < 4 as is the case for simulated Np(IV) data. Results are shown as the blue line in Figure 3b. Applying those new surface complexation data in Table S2 does not result in major changes for the resulting $\{Pu(IV)/Pu(III)\}_{surf}$ borderline (Figure 3a, bold red line). Our above conclusions remain valid.

Using the 2 SPNE SC/CE model with the surface complexation constants in Table S2 and taking into account the range of measured redox conditions (pH + pe = 11.8 ± 1.0; Figure. 3a) allows for an excellent simulation of experimental Pu sorption data over the whole pH-range investigated (Figure 2a). Decreasing R_d values at pH < 5 are nicely reproduced as a consequence of progressing reduction of Pu(IV) to Pu(III) with decreasing pH. Variations in log R_d for pH = 4.3

326 are assigned to the effect of pe rather than to a concentration effect (Fig. 2c). For $6 < pe < 8.5$,
327 Pu(III) prevails in solution whereas Pu(IV) prevails at the illite surface. This explains why log R_d
328 values lie between that of Pu(III) and Pu(IV), when they occur as single components.
329
330 **Environmental implications.** These results related to Pu(IV)/Pu(III) transition in presence
331 of illite, together with the outcome of earlier studies such as Pu(V)/Pu(IV) redox reactions in
332 aqueous kaolinite suspensions[17] or the Np(V)/Np(IV) transition in presence of illite,[13]
333 demonstrate the applicability of our approach to describe actinide redox reactions in presence of
334 mineral surfaces over a wide range of possible redox conditions where Pu(III), Pu(IV) and Pu(V)
335 may exist. A more accurate simulation of redox sensitive element behavior in near surface soil
336 systems and deep geological formations becomes possible by implementing measured pe values
337 of a given system into geochemical surface speciation calculations. Therefore, this study may
338 allow a more accurate estimation of Pu mobility in the geosphere. Because natural systems can be
339 much more complicated, containing e.g. carbonates and natural organic matter, further studies are
340 required to verify the applicability of the present approach to a wider range of geochemical
341 conditions. Our approach might also be tested for redox sensitive elements other than actinides
342 (e.g. cerium, selenium, arsenic, chromium, iron).
343
344 **ASSOCIATED CONTENT**
345 Materials and Methods: Extraction methods, Pu oxidation state analysis. Results and Discussion:
346 Thermodynamic calculations (Surface complexation, cation exchange, SIT parameters),
347 Experimental sorption data. This material is available free of charge via the Internet at
348 http://pubs.acs.org.

AUTHOR INFORMATION

Corresponding Author

* nidhu.banik@kit.edu

Present Addresses

†Ecole Nationale Supérieure de Chimie de Rennes, UMR CNRS 6226, 11 Allée de Beaulieu, F-35708 Rennes Cedex 7, France.

Groupe d'Etudes Atomiques (GEA), Ecole des Applications Militaires de l'Energie Atomique (EAMEA). BCRM Cherbourg, CC19 50115 Cherbourg-Octeville Cedex, France

Notes

The authors declare no competing financial interest.

ACKNOWLEDGEMENTS

This work was financed by the Federal Ministry of Economic Affairs and Energy (Germany) under contracts No. 02E10206 and 02E10961. The research leading to these results has received funding from the European Union's European Atomic Energy Community's (Euratom) Seventh Framework Program FP7/2007-2011 under grant agreement n° 249624 (CATCLAY project).

370 **REFERENCES**

371 (1) Altmaier, M.; Gaona, X.; Fanghanel, T. Recent advances in aqueous actinide chemistry and
372 thermodynamics. *Chemical Reviews* **2013,** *113* (2), 901-943.

373 (2) Geckeis, H.; Lutzenkirchen, J.; Polly, R.; Rabung, T.; Schmidt, M. Mineral-Water interface
374 reactions of actinides. *Chemical Reviews* **2013,** *113* (2), 1016-1062.

375 (3) Begg, J. D.; Zavarin, M.; Zhao, P. H.; Tumey, S. J.; Powell, B.; Kersting, A. B. Pu(V) and
376 Pu(IV) sorption to montmorillonite. *Environmental Science & Technology* **2013,** *47* (10), 5146-
377 5153.

378 (4) Zavarin, M.; Powell, B. A.; Bourbin, M.; Zhao, P. H.; Kersting, A. B. Np(V) and Pu(V) ion
379 exchange and surface-mediated reduction mechanisms on montmorillonite. *Environmental*
380 *Science & Technology* **2012,** *46* (5), 2692-2698.

381 (5) Tinnacher, R. M.; Begg, J. D.; Mason, H.; Ranville, J.; Powell, B. A.; Wong, J. C.; Kersting,
382 A. B.; Zavarin M. Effect of Fulvic Acid Surface Coatings on Plutonium Sorption and Desorption
383 Kinetics on Goethite. *Environmental Science & Technology* **2015**, 49 (5), 2776–2785.

384 (6) Hixon, A. E.; Powell, B. A. Observed changes in the mechanism and rates of Pu(V) reduction
385 on hematite as a function of total plutonium concentration. *Environmental Science & Technology*
386 **2014,** *48* (16), 9255-9262.

387 (7) Powell, B. A.; Fjeld, R. A.; Kaplan, D. I.; Coates, J. T.; Serkiz, S. M. $Pu(V)O_2^+$ Adsorption
388 and Reduction by Synthetic Magnetite (Fe_3O_4). *Environmental Science & Technology* **2004**, *38*,
389 6016-6024.

390 (8) Powell, B. A.; Fjeld, R. A.; Kaplan, D. I.; Coates, J. T.; Serkiz, S. M. $Pu(V)O_2^+$ adsorption
391 and reduction by synthetic hematite and goethite. *Environmental Science & Technology* **2005,** *39*
392 (7), 2107-2114.

(9) Romanchuk, A. Y.; Kalmykov, S. N.; Aliev, R. A. Plutonium sorption onto hematite colloids at femto- and nanomolar concentrations. *Radiochimica Acta* **2011**, *99*, 137-144.

(10) Romanchuk, A. Y.; Kalmykov, S. N.; Egorov, A. V.; Zubavichus, Y. V.; Shiryaev, A. A.; Batuk, O. N.; Conradson, S. D; Pankratov , D. A; Presnyakov, I. A. Formation of crystalline PuO_{2+x} $n.H_2O$ nanoparticles upon sorption of Pu(V,VI) onto hematite. *Geochimica et Cosmochimica Acta* **2013,** *121*, 29-40.

(11) Hixon, A. E.; Arai, Y.; Powell, B. A. Examination of the effect of alpha radiolysis on plutonium(V) sorption to quartz using multiple plutonium isotopes. *Journal of Colloid and Interface Science* **2013,** *403*, 105-112.

(12) Banik, N. L.; Buda, R. A.; Burger, S.; Kratz, J. V.; Trautmann, N. Sorption of tetravalent plutonium and humic substances onto kaolinite. *Radiochimica Acta* **2007,** *95*, (10), 569-575.

(13) Marsac, R.; Banik, N. L.; Lutzenkirchen, J.; Marquardt, C. M.; Dardenne, K.; Schild, D.; Rothe, J.; Diascorn, A.; Kupcik, T.; Schafer, T.; Geckeis, H. Neptunium redox speciation at the illite surface. *Geochimica et Cosmochimica Acta* **2015,** *152*, 39-51.

(14) Guillaumont, R.; Fanghänel, Th.; Fuger, J.; Grenthe, I.; Neck, V.; Palmer, D. A.; Rand, M. H. *Update on the Chemical Thermodynamics of Uranium, Neptunium, Plutonium, Americium and Technetium*; Amsterdam, **2003**.

(15) Kirsch, R.; Fellhauer, D.; Altmaier, M.; Neck, V.; Rossberg, A.; Fanghanel, T.; Charlet, L.; Scheinost, A. C. Oxidation state and local structure of plutonium reacted with magnetite, mackinawite, and chukanovite. *Environmental Science & Technology* **2011,** *45* (17), 7267-7274.

(16) Buda, R. A.; Banik, N. L.; Kratz, J. V.; Trautmann, N. Studies of the ternary systems humic substances – kaolinite – Pu(III) and Pu(IV). *Radiochimica Acta* **2008**, *96*, 657-665.

(17) Marsac, R.; Banik, N. L.; Lützenkirchen, J.; Buda, R. A.; Kratz, J. V.; Marquardt, C. M. Modeling plutonium sorption to kaolinite: Accounting for redox equilibria and the stability of surface species. *Chemical Geology* **2015,** *400*, 1-10.

(18) Choppin, G. R. Utility of oxidation state analogs in the study of plutonium behavior. *Radiochimica Acta* **1999**, *85*, 89-95.

(19) Bradbury, M. H.; Baeyens, B.; Geckeis, H.; Rabung, T. Sorption of Eu(III)/Cm(III) on Ca-montmorillonite and Na-illite. Part 2: Surface complexation modelling. *Geochimica Cosmochimica Acta* **2005**, *69*, 5403-5412.

(20) Bradbury, M. H.; Baeyens, B. Sorption modelling on illite Part I: Titration measurements and the sorption of Ni, Co, Eu and Sn. *Geochimica et Cosmochimica Acta* **2009,** *73* (4), 990-1003.

(21) Bradbury, M. H.; Baeyens, B. Sorption modelling on illite. Part II: Actinide sorption and linear free energy relationships. *Geochimica et Cosmochimica Acta* **2009,** *73* (4), 1004-1013.

(22) Marquardt, C. M.; Seibert, A.; Artinger, R.; Denecke, M. A.; Kuczewski, B.; Schild, D.; Fanghanel, T. The redox behaviour of plutonium in humic rich groundwater. *Radiochimica Acta* **2004,** *92*, (9-11), 617-623.

(23) Nitsche, H.; Roberts, K.; Xi, R. H.; Prussin, T.; Becraft, K.; Almahamid, I.; Silber, H. B.; Carpenter, S. A.; Gatti, R. C.; Novak, C. F. Long-Term plutonium solubility and speciation studies in a synthetic brine. *Radiochimica Acta* **1994,** *66-7*, 3-8.

(24) Neck, V.; Altmaier, M.; Seibert, A.; Yun, J. I.; Marquardt, C. M.; Fanghänel, Th. Solubility and redox reactions of Pu(IV) hydrous oxide: Evidence for the formation of $PuO_{2+x(s,hyd)}$. *Radiochimica Acta* **2007**, *95*, 193-207.

(25) Kinniburgh, D. G., Cooper, D. M. *PhreePlot: Creating graphical output with PHREEQC*. http://www.phreeplot.org. **2009**.

(26) Parkhurst, D. L.; Appelo, C. A. J. *User's guide to PHREEQC (Version 2) – a computer program for speciation, batch reaction, one-dimensional transport and inverse geochemical calculation*; Denver, Colorado, **1999**; PP 312.

(27) Ciavatta, L. The specific interaction theory in evaluating ionic equilibria. *Annali Di Chimica* **1980,** *70*, (11-1), 551-567.

(28) Gorgeon, L. Contribution à la modélisation physico-chimique de la rétention de radioéléments à vie longue par des matériaux argileux. *Ph.D. thesis, Université Paris 6,* **1994**.

(29) Farr, J. D.; Neu, M. P.; Schulze, R. K.; Honeyman, B. D. Plutonium uptake by brucite and hydroxylated periclase. *Journal of Alloys and Compounds* **2007**, *444*, 533-539.

(30) Bauer, A.; Berger, G. Kaolinite and smectite dissolution rate in high molar KOH solutions at 35° and 80°C. *Applied Geochemistry* **1998**, *13*, 905-916.

(31) Rabung, T.; Pierret, M. C.; Bauer, A.; Geckeis, H.; Bradbury, M. H.; Baeyens, B. Sorption of Eu(III)/Cm(III) on Ca-montmorillonite and Na-illite. Part 1: Batch sorption and time-resolved laser fluorescence spectroscopy experiments. *Geochimica Cosmochimica Acta* **2005**, *69*, 5393-5402.

(32) Finck, N.; Schlegel, M. L.; Bosbach, D. Sites of Lu(III) Sorbed to and Coprecipitated with Hectorite. *Environmental Science & Technology* **2009**, 43 (23), 8807-8812.

(33) Bradbury, M. H.; Baeyens, B. Predictive sorption modelling of Ni(II), Co(II), Eu(IIII), Th(IV) and U(VI) on MX-80 bentonite and Opalinus Clay: A “bottom-up” approach. *Applied Clay Science* **2011**, *52*, 27-33.

(34) Marques Fernandes, M; Vér, N.; Bart Baeyens, B. Predicting the uptake of Cs, Co, Ni, Eu, Th and U on argillaceous rocks using sorption models for illite. *Applied Geochemistry* **2015**, *59*, 189-199.

462 (35) Kalmykov, S. N.; Vlasova, I. E; Romanchuk, A. Y.; Zakharova, E. V.; Volkova, A. G.;
463 Presnyakov, I. A. Partitioning and speciation of Pu in the sedimentary rocks aquifer from the
464 deep liquid nuclear waste disposal. *Radiochimica Acta* **2015**, *103* (3), 175-185.
465

Figure Caption

Figure 1. pH-pe values measured in illite suspensions under anaerobic conditions. Present work: 1 week (gray diamonds) and 1 year equilibration time (black diamonds); previous investigations of the Np-illite system: white circles.[13] Large symbols indicate the samples where the supernatant was analyzed by liquid extraction ($[Pu]_{tot} = 10^{-8}$ M). The predominance pH-pe diagram for Pu in 0.1 M NaCl (solid lines) is also shown.

Figure 2. (a) Pu sorption to illite (R_d: distribution coefficient in L kg^{-1}) in 0.1 M NaCl as a function of the pH ($8\times10^{-11} < [Pu]_{tot} < 10^{-8}$ M) after 1 week (white squares) and 1 year (black diamonds) contact time. Results after 1 year are compared with overall log R_d calculated for pH + pe = 11.8 ± 1.0 (bold line; lower and upper values: dashed and dashed-dotted lines, respectively; se text for more details). (b) log-log plot of R_d versus the final aqueous Pu concentration ($[Pu]_{aq}$) for pH = 4.3 (black triangles) and pH > 5 (gray circles) after 1 year contact time. Average value and standard deviation of log R_d (5.2 ± 0.2) for pH > 5 are shown as gray solid and dashed lines, respectively. (c) Experimental and calculated log R_d values for pH = 4.3 versus pe.

Figure 3. (a) Predominance pH-pe diagram for Pu in 0.1 M NaCl with pH-pe values measured in illite suspensions after 1 year equilibration time. The bold and dashed red lines show estimated borderlines for Pu(IV)/Pu(III) redox transition at the illite surface (see text for more details). Relevant redox conditions for this study (pH+pe = 11.8 ± 1.0) are shown as straight (solid and dashed) lines. (b) Data for Pu uptake onto illite (R_d in L kg^{-1}) as a function of pH compared with model calculations for Eu(III) (green bold line), Np(IV) (dashed black line) and Pu(IV) (blue bold line) sorption based on the 2 SPNE SC/CE model.

488

489 **Figure 1**

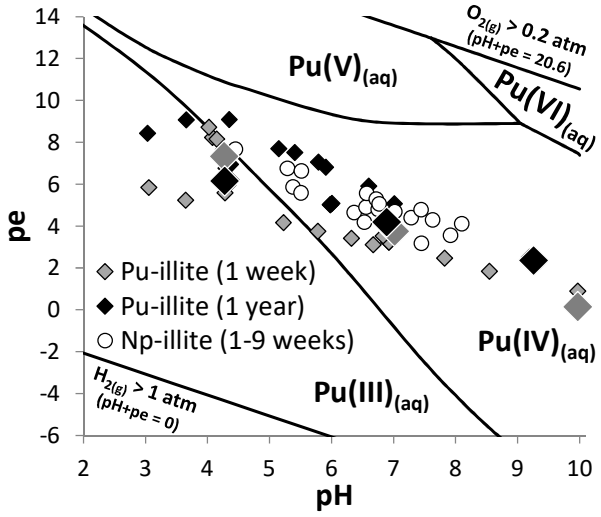

490

491

Figure 2

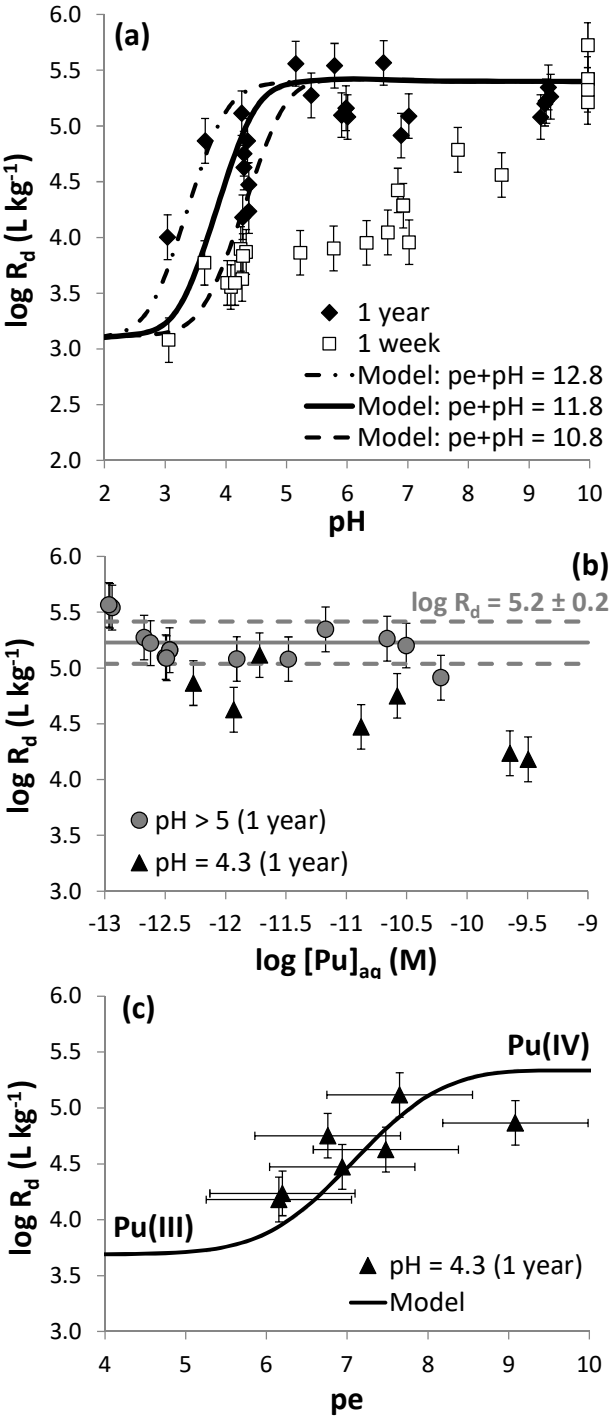

492

493

Figure 3

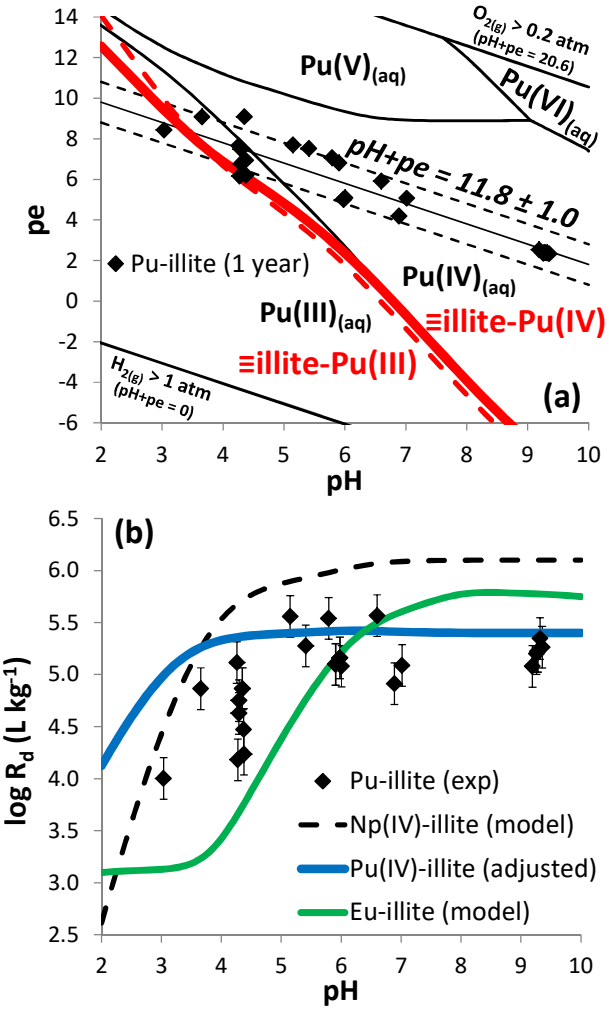

494

495

496

497

TOC/abstract

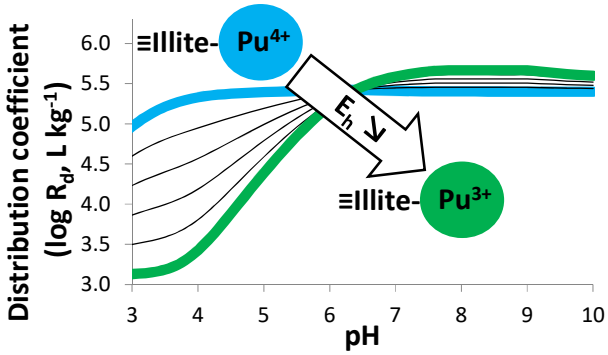

498